Bol. Soc. Paran. Mat.
©SPM – E-ISSN-2175-1188
SPM: www.spm.uem.br/bspm

(3s.) **v. 2025 (43)** : 1–28.
ISSN-0037-8712
doi:10.5269/bspm.78429

Zagreb-Type Topological Indices and Entropy Measures of Zinc Oxide and Silicate Networks

U. Vijaya Chandra Kumar*, Nagesh H. M.

ABSTRACT: Metal-organic frameworks (MOFs) are attractive porous materials created by combining organic components with metals. These materials exhibit remarkable efficiency and have diverse applications in various medical fields. Recently, zinc-based MOFs have attracted significant attention because of their effective use in biosensing, cancer therapy, and drug delivery. Due to the various applications of MOFs, topological and entropy properties also emerge as important tools for development. This paper determines the new Zagreb-type topological indices and their corresponding entropy measures for zinc oxide and silicate networks. Using Shannon's entropy model, entropy measures based on the Zagreb-type topological indices are derived. The Zagreb-type topological indices and their entropy measures are compared through numerical computations and graphical representations. The relationship between Zagreb-type topological indices and the associated entropy measures is analyzed using curve fitting and Pearson correlation analysis.

Key Words: Zagreb-type topological indices, graph entropy, zinc oxide network, zinc silicate network.

Contents

1. Introduction

Metal-organic frameworks (MOFs) have emerged as a remarkable class of crystalline materials characterized by ultrahigh porosity, with up to 90% free volume and vast internal surface areas exceeding 6,000 m^2/g. These features, combined with the exceptional tunability of both their organic and inorganic components, make MOFs highly attractive for applications in clean energy. Notable uses include gas storage, such as hydrogen and methane, and as high-capacity adsorbents for various separation processes. Moreover, their potential applications extend to membranes, thin-film devices, catalysis, and biomedical imaging, which are becoming increasingly significant. Fundamentally, MOFs exemplify the elegance of

* Corresponding author.
2010 *Mathematics Subject Classification:* 05C05, 05C12, 05C90.
Submitted August 15, 2025. Published October 29, 2025

chemical structures and the synergy of organic and inorganic chemistry, two fields often viewed as distinct. Since the 1990s, research on MOFs has grown rapidly, as shown by the large amount of research work and the expanding areas of study [1].

Metal-organic frameworks (MOFs) are a type of porous polymer constructed from metal clusters, known as Secondary Building Units (SBUs), connected to organic ligands. These frameworks can form one-, two-, or three-dimensional structures. The organic ligands also referred to as linkers, include compounds such as 1,4-benzenedicarboxylic acid (BDC). A metal-organic framework (MOF) is formally defined as a potentially porous extended structure composed of metal ions and organic linkers [2,3,4]. An extended structure is characterized by sub-units that maintain a constant ratio and are arranged in a repeating pattern. MOFs are a subset of coordination networks, which are coordination compounds extending in one dimension through repeating coordination entities, with additional cross-links between chains, loops, or spiro-links, or as structures extending through repeating entities in two or three dimensions. Furthermore, coordination networks, including MOFs, are part of the broader category of coordination polymers, defined as coordination compounds with repeating coordination entities extending in one, two, or three dimensions [5]. Most MOFs described in the literature are crystalline compounds, although amorphous MOFs [6] and other disordered phases [7] have also been reported. In most cases, the pores in MOFs remain stable even after removing guest molecules, such as solvents, and can subsequently be refilled with other substances. This unique property makes MOFs particularly appealing for applications like gas storage, including hydrogen and carbon dioxide. Also, MOFs are potentially used in gas purification, gas separation, water remediation, catalysis, conductive materials, and supercapacitors [8,9].

Topological indices serve as valuable predictive tools in quantitative structure-activity relationship (QSAR) and quantitative structure-property relationship (QSPR) studies, calculated using precise mathematical expressions [10,11,12]. Graph entropies, derived from these indices, represent structural information content and play a crucial role in assessing the stability of molecular compounds [13,14,15,16]. The mathematical modeling of metal-organic frameworks (MOFs) has primarily focused on degree- and degree-sum-based topological indices [17,18,19,20]. The emphasis was particularly on connection-based TIs, connection-based Zagreb indices, multiplicative Zagreb connection indices, and neighborhood degree sum-based topological indices. Even though these studies provide a strong basis for comprehending the behavior and structural characteristics of MOFs, more research is still required to provide a deeper understanding of the connection between topological indices and the entropy measures that go along with them. An examination of this kind might yield a more thorough comprehension of the network's functionality and stability.

1.1. Novelty and motivation

MOFs, particularly zinc-based frameworks, have gained attention for their flexibility and effectiveness in medical applications such as biosensing, cancer therapy, and drug delivery. A more complete understanding of their structural characteristics using topological indices and entropy metrics is still lacking, despite their widespread application. This paper is motivated by the need to fill this gap by offering new mathematical tools and computational methods to characterize and predict key properties of MOFs, ultimately contributing to their design and optimization for diverse applications. Metal-organic frameworks (MOFs) have many uses, making their topological and entropy properties important for their development. The Zagreb-type topological indices have strong predictive abilities [21,22]. To the best of our knowledge, no studies have explored Zagreb-type topological indices of metal-organic frameworks. This study aims to explore the fundamental relationship between structural topologies and material properties that contribute to advancements in MOF-based technologies. It introduces new Zagreb-type topological indices for zinc oxide and silicate networks. This area has seen limited exploration in the context of topological and entropy measures. The study takes a new approach by analyzing these indices using entropy measures derived from Shannon's model.

1.2. Methodology

In this paper, we analyze the structural properties of zinc oxide and silicate networks. We employ Shannon's entropy measures derived from novel information functions based on various definitions of new

Zagreb-type topological indices. A comprehensive mathematical and computational examination of these measures is carried out for the zinc oxide and silicate networks. The organization of the paper is as follows:

- Section 2 discusses the various Zagreb-type topological indices used in the study.
- Section 3 provides the computation of Zagreb-type topological indices and the corresponding entropies of zinc oxide and silicate networks.
- Section 4 compares the Zagreb-type topological indices and their corresponding entropy measures through numerical data and graphical illustrations for the zinc oxide and silicate networks $ZNOX(\alpha)$ and $ZNSL(\alpha)$ for $1 \leq \alpha \leq 100$.
- Section 5 develops optimal regression models that correlate the Zagreb-type topological indices to the associated entropies of $ZNOX(\alpha)$ and $ZNSL(\alpha)$ for $1 \leq \alpha \leq 100$.
- Section 6 computes the Pearson correlation between the Zagreb-type topological indices and their entropy measures of $ZNOX(\alpha)$ and $ZNSL(\alpha)$ for $1 \leq \alpha \leq 100$.
- Finally, Section 7 presents the conclusion with future work.

2. Preliminaries

We provide definitions for certain basic terms and symbols used throughout the work. A graph $G = (V, E)$ consists of a vertex set $V(G)$ and an edge set $E(G)$, where $|V(G)| = \phi$ and $|E(G)| = \psi$ denote the number of vertices and edges of G, respectively. The notation $\phi_1\phi_2$ denotes an edge connecting two vertices ϕ_1 and ϕ_2. An important concept in graph theory is the degree of a vertex in G. The degree of a vertex v, denoted by $d(v)$, is defined as the number of edges in G that are incident to v.

We now present various Zagreb-type topological indices [21] as follows:

1. Bi-Zagreb $BM(G) = \sum_{\phi\psi \in E(G)} d(\phi) + d(\psi) + d(\phi) \times d(\psi)$
2. Tri-Zagreb $TM(G) = \sum_{\phi\psi \in E(G)} d^2(\phi) + d^2(\psi) + d(\phi) \times d(\psi)$
3. Geometric-Bi-Zagreb $GBM(G) = \sum_{\phi\psi \in E(G)} \frac{\sqrt{d(\phi) \times d(\psi)}}{d(\phi) + d(\psi) + d(\phi) \times d(\psi)}$
4. Geometric-Tri-Zagreb $GTM(G) = \sum_{\phi\psi \in E(G)} \frac{\sqrt{d(\phi) \times d(\psi)}}{d^2(\phi) + d^2(\psi) + d(\phi) \times d(\psi)}$
5. Geometric-Harmonic $GH(G) = \sum_{\phi\psi \in E(G)} \frac{\sqrt{d(\phi) \times d(\psi)}(d(\phi) + d(\psi))}{2}$
6. Harmonic-Bi-Zagreb $HBM(G) = \sum_{\phi\psi \in E(G)} \frac{2}{(d(\phi) + d(\psi) + d(\phi) \times d(\psi))(d(\phi) + d(\psi))}$
7. Harmonic-Tri-Zagreb $HTM(G) = \sum_{\phi\psi \in E(G)} \frac{2}{(d^2(\phi) + d^2(\psi) + d(\phi) \times d(\psi))(d(\phi) + d(\psi))}$
8. Harmonic-Geometric $HG(G) = \sum_{\phi\psi \in E(G)} \frac{2}{\sqrt{d(\phi) \times d(\psi)}(d(\phi) + d(\psi))}$
9. Bi-Zagreb-Geometric $BMG(G) = \sum_{\phi\psi \in E(G)} \frac{d(\phi) + d(\psi) + d(\phi) \times d(\psi)}{\sqrt{d(\phi) \times d(\psi)}}$
10. Bi-Zagreb-Harmonic $BMH(G) = \sum_{\phi\psi \in E(G)} \frac{(d(\phi) + d(\psi) + d(\phi) \times d(\psi))(d(\phi) + d(\psi))}{2}$

11. Bi-Zagreb-Arithmetic $BMA(G) = \sum_{\phi\psi \in E(G)} \frac{2\,(d(\phi) + d(\psi) + d(\phi) \times d(\psi))}{d(\phi) + d(\psi)}$

12. Tri-Zagreb-Geometric $TMG(G) = \sum_{\phi\psi \in E(G)} \frac{d^2(\phi) + d^2(\psi) + d(\phi) \times d(\psi)}{\sqrt{d(\phi) \times d(\psi)}}$

13. Tri-Zagreb-Harmonic $TMH(G) = \sum_{\phi\psi \in E(G)} \frac{(d^2(\phi) + d^2(\psi) + d(\phi) \times d(\psi))(d(\phi) + d(\psi))}{2}$

14. Tri-Zagreb-Arithmetic $TMA(G) = \sum_{\phi\psi \in E(G)} \frac{2\left(d^2(\phi) + d^2(\psi) + d(\phi) \times d(\psi)\right)}{d(\phi) + d(\psi)}$

By defining χ as the Zagreb-type topological indices of G, it is generally expressed as:

$$\chi(G) = \sum_{e \in E(G)} \Omega(e),$$

where Ω is a structural function that characterizes the bond-additive topological index.

The idea of entropy, first introduced by Shannon [23], measures the unpredictability of information content or the uncertainty within a system. Over time, this concept was extended to graphs and chemical networks, where it evolved as a tool for quantifying structural information. In 1955, Rashevsky [24] advanced the idea of graph entropy by defining it based on vertex orbit classifications. In recent years, graph entropies have found extensive applications across diverse fields, including chemistry, biology, ecology, and sociology [25]. These measures, which associate probability distributions with graph elements such as vertices or edges, can be classified into intrinsic and extrinsic types. Various graph entropy measures have been developed [26]. Degree powers, which are significant invariants in graph theory and network science, are frequently employed as information functions for network analysis [27,28]. Dehmer [29] introduced graph entropies based on information functions to encapsulate structural information, and their properties have been widely studied. Furthermore, Estrada et al. proposed a physically meaningful entropy measure for graphs [30] and explored walk-based graph entropies [31]. Graph entropy quantifies the information content of a graph, often computed using topological indices as functions. The application of information-theoretic concepts to measure graph entropy and its extended features has enabled diverse applications in areas like structural chemistry, biology, and computer science.

As described in [32,33], the entropy based on a topological index (TI) is defined as

$$ENT_{TI(G)} = log(TI(G)) - \frac{1}{TI(G)} \sum_{e \in E(G)} \Omega(e) log(\Omega(e)) \tag{2.1}$$

The formula (2.1) determines graph entropies of zinc oxide and silicate networks.

3. Main results

In the first part of this section, analytical expressions for various Zagreb-type topological indices of zinc oxide and silicate networks are derived. Subsequently, the probabilistic entropy values for these metal-organic frameworks are calculated and presented in tabular form using the computed topological indices. Finally, the entropy values are graphically plotted and analyzed to observe the trends across different structures as determined by various topological descriptors.

The molecular structures of zinc oxide and zinc silicate networks denoted as $ZNOX(\alpha)$ and $ZNSL(\alpha)$, for growth parameter, $\alpha = 1$ are shown in Figure 1 and Figure 2, respectively.

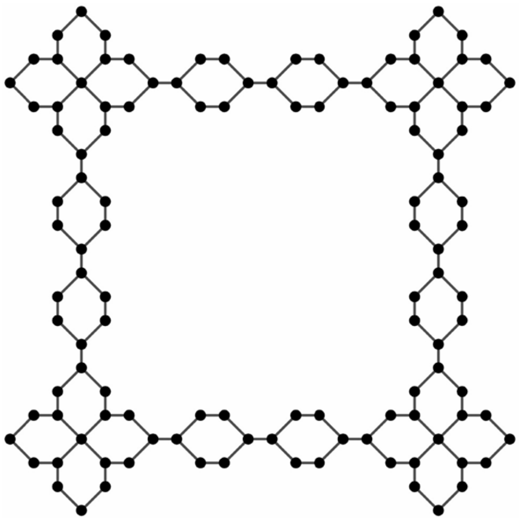

Figure 1: Building unit of $ZNOX(\alpha)$

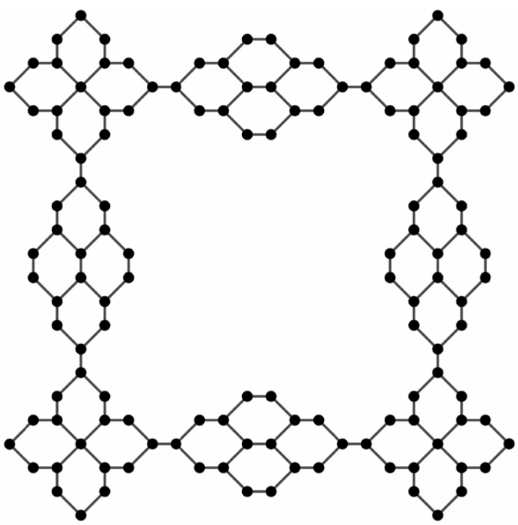

Figure 2: Building unit of $ZNSL(\alpha)$

3.1. New Zagreb-type topological indices

The total numbers of vertices and edges of $ZNOX(\alpha)$ and $ZNSL(\alpha)$ are as follows:

$$|V(ZNOX(\alpha)| = 70\alpha + 46;\ |E(ZNOX(\alpha)| = 85\alpha + 55;$$
$$|V(ZNSL(\alpha)| = 82\alpha + 50;\ |E(ZNSL(\alpha)| = 103\alpha + 61.$$

The edge sets of $ZNOX(\alpha)$ and $ZNSL(\alpha)$ are divided into four distinct classes based on the degrees of the end vertices, as shown in Table 1.

Table 1: Degree-based edge partition of $ZNOX(\alpha)$ and $ZNSL(\alpha)$

$(d(u), d(v))$	$ZNOX(\alpha)$	$ZNSL(\alpha)$
(2,2)	$16\alpha + 16$	$10\alpha + 14$
(2,3)	$52\alpha + 28$	$64\alpha + 32$
(3,3)	$9\alpha + 3$	$21\alpha + 7$
(3,4)	$8\alpha + 8$	$8\alpha + 8$

Consider the ordered pairs $(2, 2)$, $(2, 3)$, $(3, 3)$, and $(3, 4)$ representing the degrees of the end vertices for the partitions. Let Θ_{ij}, where $i \leq j$, denote the number of edges in the class C_{ij}, with i and j as the degrees of their end vertices. The values of Θ_{22}, Θ_{23}, Θ_{33}, and Θ_{34} are provided in Table 1. As explained in [34], calculating each topological index involves evaluating the function $\Omega(e)$ for one edge in each disjoint class $\{C_{22}, C_{23}, C_{33}, C_{34}\}$, multiplying these values by the corresponding total number of edges in each class, and summing the results to derive the exact analytical expression for the index.

For $e_{ij} \in C_{ij}$, we have

$$\chi(G) = \Theta_{22} \times \Omega(e_{22}) + \Theta_{23} \times \Omega(e_{23}) + \Theta_{33} \times \Omega(e_{33}) + \Theta_{34} \times \Omega(e_{34}) \tag{3.1}$$

By substituting the values Θ_{22}, Θ_{23}, Θ_{33}, and Θ_{34} corresponding to $ZNOX(\alpha)$ and $ZNSL(\alpha)$ into (2), we obtain,

$$\chi(ZNOX(\alpha)) = (16\alpha + 16)\Omega(e_{22}) + (52\alpha + 28)\Omega(e_{23}) + (9\alpha + 3)\Omega(e_{33}) + (8\alpha + 8)\Omega(e_{34})$$

$$\chi(ZNSL(\alpha)) = (10\alpha + 14)\Omega(e_{22}) + (64\alpha + 32)\Omega(e_{23}) + (21\alpha + 7)\Omega(e_{33}) + (8\alpha + 8)\Omega(e_{34})$$

Finally, substituting the values of $\Omega(e_{22})$, $\Omega(e_{23})$, $\Omega(e_{33})$, and $\Omega(e_{34})$ in these results, we obtain the following Theorems 1 - 2.

Theorem 1 *Let G be a zinc oxide network $ZNOX(\alpha)$ of dimension $\alpha \geq 1$. Then*

1. $BM(G) = 987\alpha + 633$
2. $TM(G) = 1719\alpha + 1101$
3. $GBM(G) = \frac{29\alpha}{5} + \frac{2\sqrt{3}(8\alpha+8)}{19} + \frac{\sqrt{6}(52\alpha+28)}{11} + \frac{23}{5}$
4. $GTM(G) = \frac{11\alpha}{3} + \frac{2\sqrt{3}(8\alpha+8)}{37} + \frac{\sqrt{6}(52\alpha+28)}{19} + 3$
5. $GH(G) = 145\alpha + 7\sqrt{3}(8\alpha + 8) + \frac{5\sqrt{2}\sqrt{3}(52\alpha+28)}{2} + 91$
6. $HBM(G) = \frac{4698\alpha}{1463} + \frac{48392}{21945}$
7. $HTM(G) = \frac{428339\alpha}{221445} + \frac{900143}{664335}$
8. $HG(G) = 5\alpha + \frac{\sqrt{3}(8\alpha+8)}{21} + \frac{\sqrt{6}(52\alpha+28)}{30} + \frac{13}{3}$
9. $BMG(G) = 109\alpha + \frac{19\sqrt{3}(8\alpha+8)}{6} + \frac{11\sqrt{6}(52\alpha+28)}{6} + 79$
10. $BMH(G) = 2623\alpha + 1693$
11. $BMA(G) = \frac{13343\alpha}{35} + \frac{8597}{35}$
12. $TMG(G) = 177\alpha + \frac{37\sqrt{3}(8\alpha+8)}{6} + \frac{19\sqrt{6}(52\alpha+28)}{6} + 123$
13. $TMH(G) = 4619\alpha + 2993$
14. $TMA(G) = \frac{22987\alpha}{35} + \frac{14713}{35}$

Theorem 2 *Let G be a zinc silicate network $ZNSL(\alpha)$ of dimension $\alpha \geq 1$. Then*

1. $BM(G) = 1251\alpha + 721$
2. $TM(G) = 2199\alpha + 1261$
3. $GBM(G) = (\frac{67\alpha}{10}) + \frac{2\cdot\sqrt{3}\cdot(8\alpha+8)}{19} + \frac{\sqrt{6}\cdot(64\alpha+32)}{11} + \frac{49}{10}$
4. $GTM(G) = 4\alpha + \frac{2\cdot\sqrt{3}\cdot(8\alpha+8)}{37} + \frac{\sqrt{6}\cdot(64\alpha+32)}{19} + \frac{28}{9}$
5. $GH(G) = 229\alpha + 7\sqrt{3}(8\alpha+8) + \frac{5\sqrt{2}\sqrt{3}(64\alpha+32)}{2} + 119$
6. $HBM(G) = \frac{621349\alpha}{175560} + \frac{1218997}{526680}$
7. $HTM(G) = \frac{5540741\alpha}{2657340} + \frac{11202389}{7972020}$
8. $HG(G) = \frac{29\alpha}{6} + \frac{\sqrt{3}(8\alpha+8)}{7} + \frac{\sqrt{6}(64\alpha+32)}{5} + \frac{77}{18}$
9. $BMG(G) = 145\alpha + \frac{19\sqrt{3}(8\alpha+8)}{6} + \frac{11\sqrt{6}(64\alpha+32)}{6} + 91$
10. $BMH(G) = 3397\alpha + 1951$
11. $BMA(G) = \frac{16451\alpha}{35} + \frac{9633}{35}$
12. $TMG(G) = 249\alpha + \frac{37\sqrt{3}(8\alpha+8)}{6} + \frac{19\sqrt{6}(64\alpha+32)}{6} + 147$
13. $TMH(G) = 6017\alpha + 3459$
14. $TMA(G) = \frac{28699\alpha}{35} + \frac{16617}{35}$

3.2. Calculating Zagreb-type topological index-based entropy values

The calculation of entropy values following Shannon's approach by defining the probability function using Zagreb-type topological indices is explained in this section. The entropy values are computed using (2.1). The method is demonstrated by calculating the entropy value for $ZNOX(\alpha)$ using the Bi-Zagreb index.

Let G denote the zinc oxide network $ZNOX(\alpha)$. Then the Bi-Zagreb entropy $ENT_{BM(G)}$ is derived using (2.1) and Table 1 as follows:

$$\begin{aligned} ENT_{BM(G)} &= \log(BM(G)) - \frac{1}{BM(G)}\left[\sum_{e\in E(G)} \Omega(e)\log(\Omega(e))\right] \\ &= \log(BM(G)) - \frac{1}{BM(G)}[(16\alpha+16)(8)\log(8) \\ &+(52\alpha+28)(11)\log(11) + (9\alpha+3)(15)\log(15) + (8\alpha+8)(19)\log(19)] \end{aligned}$$

The general entropy expression for zinc oxide and silicate networks would be too lengthy to present as theorems. One can easily derive the corresponding Zagreb-type-based entropy expressions for each topological index using the method outlined above. Tables 2-5 present the numerical values of different Zagreb-type topological indices and entropies for zinc oxide and silicate networks.

$[\alpha]$	$BM(G)$	$TM(G)$	$GBM(G)$	$GTM(G)$	$GH(G)$	$HBM(G)$	$HTM(G)$
1	1620	2820	31.132	18.478	919.888	5.416	3.289
2	2607	4539	49.970	29.598	1480.316	8.628	5.224
3	3594	6258	68.808	40.717	2040.745	11.839	7.158
4	4581	7977	87.646	51.837	2601.173	15.050	9.092
5	5568	9696	106.484	62.956	3161.602	18.261	11.026
6	6555	11415	125.321	74.076	3722.030	21.472	12.961
7	7542	13134	144.159	85.195	4282.459	24.684	14.895
8	8529	14853	162.997	96.315	4842.887	27.895	16.829
9	9516	16572	181.835	107.435	5403.316	31.106	18.764
10	10503	18291	200.673	118.554	5963.744	34.317	20.698
11	11490	20010	219.511	129.674	6524.173	37.528	22.632
12	12477	21729	238.349	140.793	7084.601	40.740	24.566
13	13464	23448	257.187	151.913	7645.030	43.951	26.501
14	14451	25167	276.025	163.032	8205.458	47.162	28.435
15	15438	26886	294.863	174.152	8765.887	50.373	30.369
16	16425	28605	313.701	185.271	9326.315	53.585	32.304
17	17412	30324	332.539	196.391	9886.744	56.796	34.238
18	18399	32043	351.377	207.510	10447.172	60.007	36.172
19	19386	33762	370.215	218.630	11007.601	63.218	38.106
20	20373	35481	389.053	229.749	11568.029	66.429	40.041
21	21360	37200	407.891	240.869	12128.458	69.641	41.975
22	22347	38919	426.729	251.988	12688.886	72.852	43.909
23	23334	40638	445.567	263.108	13249.315	76.063	45.844
24	24321	42357	464.405	274.227	13809.743	79.274	47.778
25	25308	44076	483.243	285.347	14370.172	82.485	49.712
26	26295	45795	502.081	296.467	14930.600	85.697	51.647
27	27282	47514	520.919	307.586	15491.029	88.908	53.581
28	28269	49233	539.757	318.706	16051.457	92.119	55.515
29	29256	50952	558.595	329.825	16611.886	95.330	57.449
30	30243	52671	577.433	340.945	17172.314	98.541	59.384

Table 2(A)

$[\alpha]$	$HG(G)$	$BMG(G)$	$BMH(G)$	$BMA(G)$	$TMG(G)$	$TMH(G)$	$TMA(G)$
1	17.185	635.016	4316	626.857	1091.433	7612	1077.143
2	27.091	1021.412	6939	1008.086	1757.230	12231	1733.914
3	36.996	1407.809	9562	1389.314	2423.027	16850	2390.686
4	46.902	1794.206	12185	1770.543	3088.825	21469	3047.457
5	56.807	2180.602	14808	2151.771	3754.622	26088	3704.229
6	66.713	2566.999	17431	2533.000	4420.419	30707	4361.000
7	76.619	2953.396	20054	2914.229	5086.216	35326	5017.771
8	86.524	3339.792	22677	3295.457	5752.013	39945	5674.543
9	96.430	3726.189	25300	3676.686	6417.810	44564	6331.314
10	106.335	4112.586	27923	4057.914	7083.607	49183	6988.086
11	116.241	4498.982	30546	4439.143	7749.405	53802	7644.857
12	126.147	4885.379	33169	4820.371	8415.202	58421	8301.629
13	136.052	5271.775	35792	5201.600	9080.999	63040	8958.400
14	145.958	5658.172	38415	5582.829	9746.796	67659	9615.171
15	155.864	6044.569	41038	5964.057	10412.593	72278	10271.943
16	165.769	6430.965	43661	6345.286	11078.390	76897	10928.714
17	175.675	6817.362	46284	6726.514	11744.187	81516	11585.486
18	185.580	7203.759	48907	7107.743	12409.985	86135	12242.257
19	195.486	7590.155	51530	7488.971	13075.782	90754	12899.029
20	205.392	7976.552	54153	7870.200	13741.579	95373	13555.800
21	215.297	8362.949	56776	8251.429	14407.376	99992	14212.571
22	225.203	8749.345	59399	8632.657	15073.173	104611	14869.343
23	235.108	9135.742	62022	9013.886	15738.970	109230	15526.114
24	245.014	9522.139	64645	9395.114	16404.768	113849	16182.886
25	254.920	9908.535	67268	9776.343	17070.565	118468	16839.657
26	264.825	10294.932	69891	10157.571	17736.362	123087	17496.429
27	274.731	10681.328	72514	10538.800	18402.159	127706	18153.200
28	284.636	11067.725	75137	10920.029	19067.956	132325	18809.971
29	294.542	11454.122	77760	11301.257	19733.753	136944	19466.743
30	304.448	11840.518	80383	11682.486	20399.550	141563	20123.514

Table 2(B)

Table 2(A-B): Calculated values of Zagreb-type topological indices of the zinc oxide network $ZNOX(\alpha)$ for $1 \leq \alpha \leq 30$.

[α]	$ENT_{BM(G)}$	$ENT_{TM(G)}$	$ENT_{GBM(G)}$	$ENT_{GTM(G)}$	$ENT_{GH(G)}$	$ENT_{HBM(G)}$	$ENT_{HTM(G)}$
1	4.906	4.882	4.938	4.928	5.398	4.867	4.836
2	5.382	5.360	5.412	5.403	5.841	5.344	5.315
3	5.703	5.682	5.733	5.724	6.147	5.666	5.637
4	5.946	5.925	5.975	5.966	6.381	5.909	5.880
5	6.141	6.121	6.170	6.161	6.570	6.105	6.076
6	6.304	6.284	6.333	6.324	6.730	6.268	6.239
7	6.445	6.424	6.473	6.464	6.867	6.408	6.380
8	6.568	6.548	6.596	6.587	6.988	6.532	6.503
9	6.677	6.657	6.706	6.697	7.096	6.641	6.613
10	6.776	6.756	6.804	6.796	7.193	6.740	6.711
11	6.866	6.846	6.894	6.885	7.282	6.830	6.801
12	6.948	6.928	6.976	6.968	7.363	6.912	6.884
13	7.024	7.004	7.053	7.044	7.438	6.988	6.960
14	7.095	7.075	7.123	7.115	7.508	7.059	7.031
15	7.161	7.141	7.189	7.181	7.574	7.125	7.097
16	7.223	7.203	7.251	7.243	7.635	7.187	7.159
17	7.282	7.262	7.310	7.301	7.693	7.246	7.217
18	7.337	7.317	7.365	7.356	7.748	7.301	7.273
19	7.389	7.369	7.417	7.408	7.800	7.353	7.325
20	7.439	7.419	7.467	7.458	7.849	7.403	7.375
21	7.486	7.466	7.514	7.505	7.896	7.450	7.422
22	7.531	7.511	7.559	7.550	7.941	7.495	7.467
23	7.574	7.555	7.602	7.594	7.984	7.539	7.510
24	7.616	7.596	7.644	7.635	8.025	7.580	7.552
25	7.656	7.636	7.683	7.675	8.065	7.620	7.592
26	7.694	7.674	7.722	7.713	8.103	7.658	7.630
27	7.731	7.711	7.759	7.750	8.139	7.695	7.667
28	7.766	7.747	7.794	7.786	8.175	7.731	7.702
29	7.801	7.781	7.828	7.820	8.209	7.765	7.737
30	7.834	7.814	7.862	7.853	8.242	7.798	7.770

3(A)

$[\alpha]$	$ENT_{HG(G)}$	$ENT_{BMG(G)}$	$ENT_{BMH(G)}$	$ENT_{BMA(G)}$	$ENT_{TMG(G)}$	$ENT_{TMH(G)}$	$ENT_{TMA(G)}$
1	4.804	4.937	4.841	4.937	4.927	4.804	4.967
2	5.282	5.412	5.321	5.412	5.402	5.286	5.443
3	5.604	5.732	5.643	5.732	5.723	5.610	5.764
4	5.847	5.975	5.887	5.975	5.966	5.854	6.007
5	6.043	6.170	6.083	6.170	6.161	6.050	6.202
6	6.206	6.333	6.246	6.333	6.324	6.214	6.365
7	6.347	6.473	6.387	6.473	6.464	6.355	6.505
8	6.470	6.596	6.510	6.596	6.587	6.478	6.628
9	6.579	6.705	6.620	6.705	6.697	6.588	6.738
10	6.678	6.804	6.719	6.804	6.795	6.687	6.837
11	6.768	6.894	6.809	6.894	6.885	6.777	6.926
12	6.851	6.976	6.891	6.976	6.967	6.860	7.009
13	6.927	7.052	6.967	7.052	7.044	6.936	7.085
14	6.998	7.123	7.038	7.123	7.114	7.007	7.156
15	7.064	7.189	7.104	7.189	7.180	7.073	7.222
16	7.126	7.251	7.166	7.251	7.242	7.135	7.284
17	7.184	7.309	7.225	7.309	7.301	7.194	7.342
18	7.239	7.364	7.280	7.364	7.356	7.249	7.397
19	7.292	7.417	7.332	7.417	7.408	7.301	7.450
20	7.341	7.466	7.382	7.466	7.458	7.351	7.499
21	7.389	7.514	7.429	7.514	7.505	7.398	7.547
22	7.434	7.559	7.475	7.559	7.550	7.443	7.592
23	7.477	7.602	7.518	7.602	7.593	7.487	7.635
24	7.519	7.643	7.559	7.643	7.635	7.528	7.676
25	7.558	7.683	7.599	7.683	7.675	7.568	7.716
26	7.597	7.721	7.637	7.721	7.713	7.606	7.754
27	7.634	7.758	7.674	7.758	7.750	7.643	7.791
28	7.669	7.794	7.710	7.794	7.785	7.679	7.827
29	7.703	7.828	7.744	7.828	7.820	7.713	7.861
30	7.737	7.861	7.777	7.861	7.853	7.746	7.894

3(B)

Table 3(A-B): Calculated values of entropy measures of the zinc oxide network $ZNOX(\alpha)$ for $1 \leq \alpha \leq 30$.

[α]	$BM(G)$	$TM(G)$	$GBM(G)$	$GTM(G)$	$GH(G)$	$HBM(G)$	$HTM(G)$
1	1972	3460	35.895	20.985	1129.867	5.854	3.490
2	3223	5659	58.305	33.985	1847.780	9.393	5.575
3	4474	7858	80.715	46.985	2565.694	12.932	7.660
4	5725	10057	103.125	59.985	3283.607	16.471	9.745
5	6976	12256	125.535	72.985	4001.520	20.011	11.831
6	8227	14455	147.945	85.985	4719.433	23.550	13.916
7	9478	16654	170.355	98.985	5437.346	27.089	16.001
8	10729	18853	192.766	111.985	6155.260	30.628	18.086
9	11980	21052	215.176	124.985	6873.173	34.168	20.171
10	13231	23251	237.586	137.985	7591.086	37.707	22.256
11	14482	25450	259.996	150.985	8309.000	41.246	24.341
12	15733	27649	282.406	163.985	9026.912	44.785	26.426
13	16984	29848	304.816	176.985	9744.826	48.325	28.511
14	18235	32047	327.226	189.985	10462.739	51.864	30.596
15	19486	34246	349.637	202.985	11180.652	55.403	32.681
16	20737	36445	372.047	215.985	11898.565	58.942	34.766
17	21988	38644	394.457	228.984	12616.478	62.482	36.851
18	23239	40843	416.867	241.984	13334.392	66.021	38.936
19	24490	43042	439.277	254.984	14052.305	69.560	41.022
20	25741	45241	461.687	267.984	14770.218	73.099	43.107
21	26992	47440	484.097	280.984	15488.131	76.639	45.192
22	28243	49639	506.508	293.984	16206.045	80.178	47.277
23	29494	51838	528.918	306.983	16923.958	83.717	49.362
24	30745	54037	551.328	319.983	17641.871	87.256	51.447
25	31996	56236	573.738	332.983	18359.784	90.796	53.532
26	33247	58435	596.148	345.983	19077.697	94.335	55.617
27	34498	60634	618.558	358.983	19795.611	97.874	57.702
28	35749	62833	640.968	371.983	20513.524	101.413	59.787
29	37000	65032	663.379	384.983	21231.437	104.952	61.872
30	38251	67231	685.789	397.983	21949.350	108.492	63.957

4(A)

$[\alpha]$	$HG(G)$	$BMG(G)$	$BMH(G)$	$BMA(G)$	$TMG(G)$	$TMH(G)$	$TMA(G)$
1	60.100	754.867	5348	745.257	1311.541	9476	1294.743
2	98.267	1231.153	8745	1215.286	2142.418	15493	2114.714
3	136.433	1707.438	12142	1685.314	2973.296	21510	2934.686
4	174.599	2183.724	15539	2155.343	3804.174	27527	3754.657
5	212.765	2660.009	18936	2625.371	4635.052	33544	4574.629
6	250.932	3136.295	22333	3095.400	5465.929	39561	5394.600
7	289.098	3612.580	25730	3565.429	6296.807	45578	6214.571
8	327.264	4088.865	29127	4035.457	7127.685	51595	7034.543
9	365.431	4565.151	32524	4505.486	7958.563	57612	7854.514
10	403.597	5041.436	35921	4975.514	8789.440	63629	8674.486
11	441.763	5517.722	39318	5445.543	9620.318	69646	9494.457
12	479.929	5994.007	42715	5915.571	10451.196	75663	10314.429
13	518.096	6470.292	46112	6385.600	11282.074	81680	11134.400
14	556.262	6946.578	49509	6855.629	12112.951	87697	11954.371
15	594.428	7422.863	52906	7325.657	12943.829	93714	12774.343
16	632.595	7899.149	56303	7795.686	13774.707	99731	13594.314
17	670.761	8375.434	59700	8265.714	14605.585	105748	14414.286
18	708.927	8851.720	63097	8735.743	15436.463	111765	15234.257
19	747.093	9328.005	66494	9205.771	16267.340	117782	16054.229
20	785.260	9804.290	69891	9675.800	17098.218	123799	16874.200
21	823.426	10280.576	73288	10145.829	17929.096	129816	17694.171
22	861.592	10756.861	76685	10615.857	18759.974	135833	18514.143
23	899.759	11233.147	80082	11085.886	19590.851	141850	19334.114
24	937.925	11709.432	83479	11555.914	20421.729	147867	20154.086
25	976.091	12185.717	86876	12025.943	21252.607	153884	20974.057
26	1014.258	12662.003	90273	12495.971	22083.485	159901	21794.029
27	1052.424	13138.288	93670	12966.000	22914.362	165918	22614.000
28	1090.590	13614.574	97067	13436.029	23745.240	171935	23433.971
29	1128.756	14090.859	100464	13906.057	24576.118	177952	24253.943
30	1166.923	14567.145	103861	14376.086	25406.996	183969	25073.914

4(B)

Table 4(A-B): Calculated values of Zagreb-type topological indices of the zinc silicate network $ZNSL(\alpha)$ for $1 \leq \alpha \leq 30$.

[α]	$ENT_{BM(G)}$	$ENT_{TM(G)}$	$ENT_{GBM(G)}$	$ENT_{GTM(G)}$	$ENT_{GH(G)}$	$ENT_{HBM(G)}$	$ENT_{HTM(G)}$
1	5.070	5.052	5.096	5.088	5.051	5.031	5.003
2	5.559	5.543	5.584	5.577	5.541	5.523	5.497
3	5.886	5.871	5.910	5.903	5.869	5.851	5.826
4	6.132	6.117	6.156	6.149	6.116	6.098	6.073
5	6.330	6.315	6.353	6.346	6.313	6.295	6.271
6	6.494	6.480	6.518	6.511	6.478	6.460	6.437
7	6.636	6.621	6.659	6.652	6.620	6.602	6.578
8	6.760	6.745	6.783	6.776	6.744	6.726	6.703
9	6.870	6.856	6.893	6.886	6.854	6.836	6.813
10	6.969	6.955	6.992	6.985	6.953	6.936	6.913
11	7.059	7.045	7.082	7.076	7.043	7.026	7.003
12	7.142	7.128	7.165	7.158	7.126	7.109	7.086
13	7.219	7.205	7.241	7.235	7.203	7.185	7.162
14	7.290	7.276	7.312	7.306	7.274	7.257	7.234
15	7.356	7.342	7.378	7.372	7.340	7.323	7.300
16	7.418	7.404	7.441	7.434	7.402	7.385	7.362
17	7.477	7.463	7.499	7.493	7.461	7.444	7.421
18	7.532	7.518	7.554	7.548	7.516	7.499	7.476
19	7.584	7.570	7.607	7.601	7.569	7.552	7.529
20	7.634	7.620	7.657	7.650	7.618	7.601	7.579
21	7.682	7.668	7.704	7.698	7.666	7.649	7.626
22	7.727	7.713	7.749	7.743	7.711	7.694	7.671
23	7.770	7.756	7.793	7.786	7.755	7.737	7.715
24	7.812	7.798	7.834	7.828	7.796	7.779	7.756
25	7.852	7.838	7.874	7.868	7.836	7.819	7.796
26	7.890	7.876	7.912	7.906	7.874	7.857	7.835
27	7.927	7.913	7.949	7.943	7.911	7.894	7.872
28	7.963	7.949	7.985	7.979	7.947	7.930	7.907
29	7.997	7.983	8.019	8.013	7.981	7.964	7.942
30	8.030	8.016	8.052	8.046	8.015	7.998	7.975

5(A)

$[\alpha]$	$ENT_{HG(G)}$	$ENT_{BMG(G)}$	$ENT_{BMH(G)}$	$ENT_{BMA(G)}$	$ENT_{TMG(G)}$	$ENT_{TMH(G)}$	$ENT_{TMA(G)}$
1	4.990	5.096	5.017	5.096	5.088	4.990	5.088
2	5.486	5.584	5.510	5.584	5.577	5.485	5.576
3	5.816	5.910	5.839	5.910	5.903	5.815	5.903
4	6.064	6.156	6.086	6.155	6.149	6.063	6.149
5	6.262	6.353	6.284	6.353	6.346	6.261	6.346
6	6.428	6.517	6.449	6.517	6.511	6.426	6.511
7	6.570	6.659	6.591	6.658	6.652	6.568	6.652
8	6.694	6.782	6.715	6.782	6.776	6.692	6.776
9	6.805	6.892	6.825	6.892	6.886	6.803	6.886
10	6.905	6.992	6.925	6.991	6.985	6.902	6.985
11	6.995	7.082	7.015	7.082	7.076	6.993	7.075
12	7.078	7.165	7.098	7.164	7.159	7.076	7.158
13	7.155	7.241	7.175	7.241	7.235	7.152	7.235
14	7.226	7.312	7.246	7.312	7.306	7.224	7.306
15	7.293	7.378	7.312	7.378	7.372	7.290	7.372
16	7.355	7.440	7.374	7.440	7.434	7.352	7.434
17	7.414	7.499	7.433	7.499	7.493	7.411	7.493
18	7.469	7.554	7.488	7.554	7.548	7.466	7.548
19	7.522	7.607	7.541	7.606	7.601	7.519	7.600
20	7.571	7.656	7.590	7.656	7.650	7.569	7.650
21	7.619	7.704	7.638	7.704	7.698	7.616	7.698
22	7.664	7.749	7.683	7.749	7.743	7.661	7.743
23	7.708	7.792	7.727	7.792	7.786	7.705	7.786
24	7.749	7.834	7.768	7.834	7.828	7.746	7.828
25	7.789	7.874	7.808	7.874	7.868	7.786	7.868
26	7.828	7.912	7.846	7.912	7.906	7.825	7.906
27	7.865	7.949	7.883	7.949	7.943	7.862	7.943
28	7.900	7.985	7.919	7.984	7.979	7.897	7.978
29	7.935	8.019	7.953	8.019	8.013	7.932	8.013
30	7.968	8.052	7.987	8.052	8.046	7.965	8.046

5(B)

Table 5(A-B): Calculated values of entropy measures of the zinc silicate network $ZNSL(\alpha)$ for $1 \leq \alpha \leq 30$.

4. Comparison through numerical and graphical demonstrations

Applications of graph entropy can be seen in fields such as information theory, computer science, chemistry, biology, and drug research. These molecular descriptors are helpful for researchers as they provide numerical data and visual representations. In this section, we compute the comparison of the Zagreb-type topological indices and corresponding entropy measures through numerical computation and 2-D line plots. Tables 2-5 show the numerical values of Zagreb-type topological indices and entropy measures of $ZNOX(\alpha)$ and $ZNSL(\alpha)$ for $1 \leq \alpha \leq 30$. Figure 3 and Figure 4 show 2-D line plots of Zagreb-type topological indices and entropy measures of $ZNOX(\alpha)$ and $ZNSL(\alpha)$ for $1 \leq \alpha \leq 100$. Figures 5 and 6 show the Pearson correlation between the indices and entropy measures of $ZNOX(\alpha)$ and $ZNSL(\alpha)$ for $1 \leq \alpha \leq 100$.

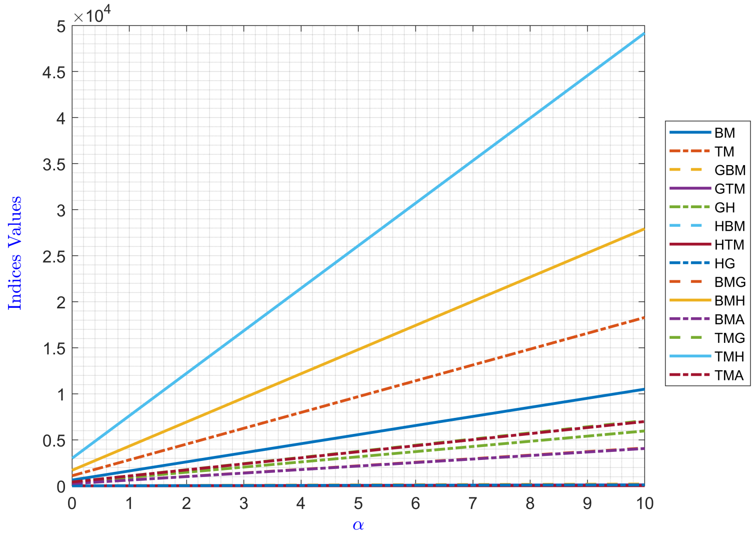

(a) Graphical representation of Zagreb-type topological indices of $ZNOX(\alpha)$ for $1 \leq \alpha \leq 100$

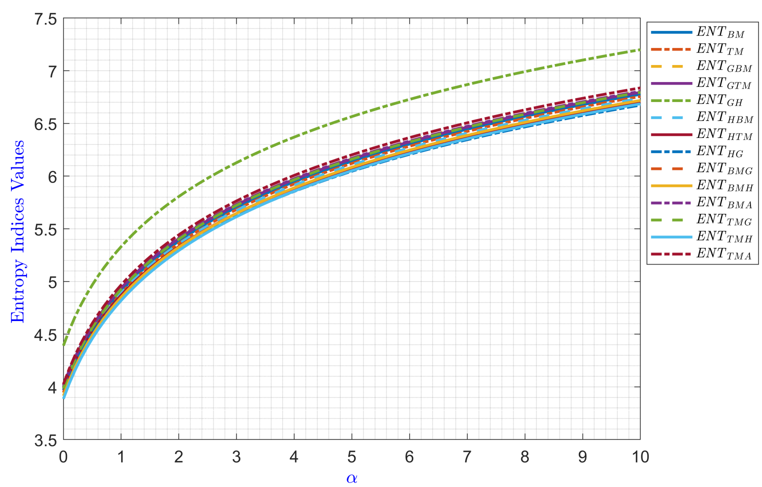

(b) Graphical representation of Zagreb-type topological indices-based entropy measures of $ZNOX(\alpha)$ for $1 \leq \alpha \leq 100$

Figure 3: (a) Graphical representation of Zagreb-type topological indices of $ZNOX(\alpha)$ for $1 \leq \alpha \leq 100$. (b) Graphical representation of the corresponding entropy measures of $ZNOX(\alpha)$ for $1 \leq \alpha \leq 100$.

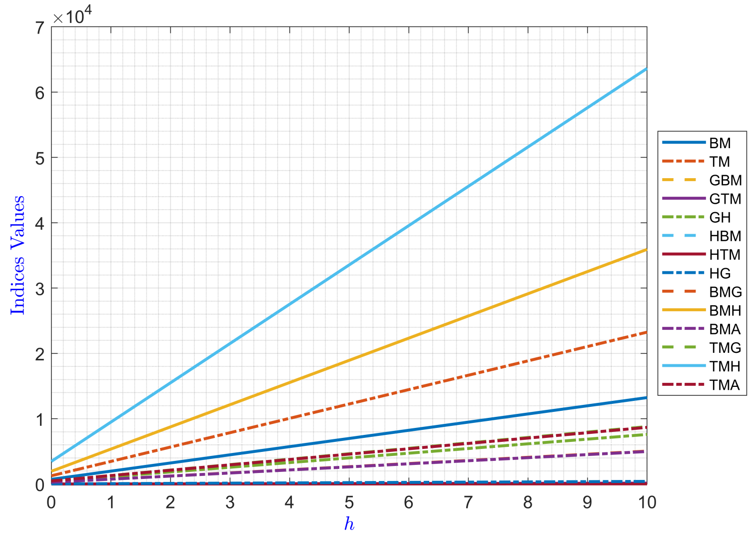

(a) Graphical representation of Zagreb-type topological indices of $ZNSL(\alpha)$ for $1 \leq \alpha \leq 100$

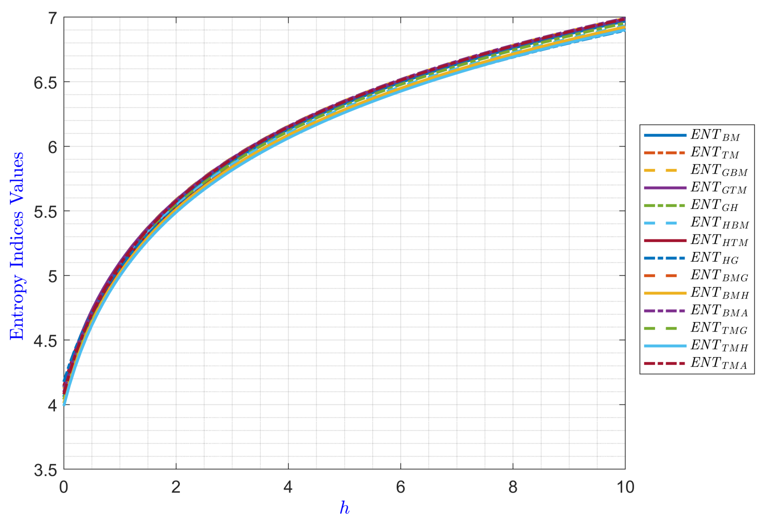

(b) Graphical representation of Zagreb-type topological indices-based entropy measures of $ZNSL(\alpha)$ for $1 \leq \alpha \leq 100$

Figure 4: (a). Graphical representation of Zagreb-type topological indices of $ZNSL(\alpha)$ for $1 \leq \alpha \leq 100$. (b). Graphical representation of the corresponding entropy measures of $ZNSL(\alpha)$ for $1 \leq \alpha \leq 100$

The following observation can be made from the data presented in Tables 2-5 and Figures 3-4.

Observation 4.1 As α increases, the Zagreb-type topological indices and the corresponding entropy measures for $ZNOX(\alpha)$ and $ZNSL(\alpha)$ also increase, demonstrating that these parameters are directly related.

5. Curve fitting between Zagreb-type topological indices and entropy measures

One of the most popular and successful data analysis techniques is curve fitting. To create the best-fit relationship model, it is used to examine the relationship between one or more independent variables and a dependent variable. There are several approaches to curve fitting, including polynomial, linear, rational, and power methods. The power-2 regression model is employed to perform this data analysis. The power-2 regression model is a type of non-linear regression model where the relationship between the independent variable x and the dependent variable y is expressed in the form:

$$y = ax^b + c,$$

where a is the scaling factor, which adjusts the overall magnitude of the curve; b is the power or exponent, which determines the relationship between x and y; and c is the intercept, which shifts the curve vertically. It is commonly used when there is a non-linear decrease or increase in the rate of change of y for x.

The sum of square error (SSE), the root mean square error (RMSE), and the squared correlation coefficient (R^2) are the statistical measurements used in the analysis. A low RMSE value (nearer to 0) and a high R^2 value (closer to 1) show that the regression lines fit the data, which are characteristics of an efficient model. Tables 6 and 7 show the statistical measurements for the zinc oxide and silicate networks, respectively, calculated using the statistics derived from these fits.

Below is the power-2 regression model used to determine the relationship between Zagreb-type topological indices and the corresponding entropy measures of $ZNOX(\alpha)$ and $ZNSL(\alpha)$ for $1 \leq \alpha \leq 100$.

5.1. Zinc oxide network $ZNOX(\alpha)$

1. General model power-2: $ENT_{BM(G)} = p_1 \cdot BM^{q_1} + r_1$, where the coefficients (with 95% confidence bounds (CB)) are $p_1 = -3669$ with CB $(-4006, -3333)$, $q_1 = -0.0002733$ with CB $(-0.0002984, -0.0002482)$, and $r_1 = 3667$ with CB $(3330, 4004)$.

2. General model power-2: $ENT_{TM(G)} = p_2 \cdot TM^{q_2} + r_2$, where the coefficients (with 95% confidence bounds (CB)) are $p_2 = -1131$ with CB $(-1234, -1028)$, $q_2 = -0.000893$ with CB $(-0.0009751, -0.0008109)$, and $r_2 = 1128$ with CB $(1025, 1231)$.

3. General model power-2: $ENT_{GBM(G)} = p_3 \cdot GBM^{q_3} + r_3$, where the coefficients (with 95% confidence bounds (CB)) are $p_3 = -1326$ with CB $(-1447, -1205)$, $q_3 = -0.000758$ with CB $(-0.0008275, -0.0006884)$, and $r_3 = 1327$ with CB $(1206, 1448)$.

4. General model power-2: $ENT_{GTM(G)} = p_4 \cdot GTM^{q_4} + r_4$, where the coefficients (with 95% confidence bounds (CB)) are $p_4 = -481.5$ with CB $(-525.1, -437.9)$, $q_4 = -0.002103$ with CB $(-0.002295, -0.00191)$, and $r_4 = 483.5$ with CB $(439.9, 527)$.

5. General model power-2: $ENT_{GH(G)} = p_5 \cdot GH^{q_5} + r_5$, where the coefficients (with 95% confidence bounds (CB)) are $p_5 = 48.74$ with CB $(43.45, 54.03)$, $q_5 = 0.01732$ with CB $(0.01569, 0.01895)$, and $r_5 = -49.46$ with CB $(-54.81, -44.11)$.

6. General model power-2: $ENT_{HBM(G)} = p_6 \cdot HBM^{q_6} + r_6$, where the coefficients (with 95% confidence bounds (CB)) are $p_6 = -166.7$ with CB $(-181.5, -151.9)$, $q_6 = -0.006173$ with CB $(-0.006733, -0.005614)$, and $r_6 = 169.8$ with CB $(155.1, 184.6)$.

7. General model power-2: $ENT_{HTM(G)} = p_7 \cdot HTM^{q_7} + r_7$, where the coefficients (with 95% confidence bounds (CB)) are $p_7 = -124.8$ with CB $(-135.7, -113.8)$, $q_7 = -0.008296$ with CB $(-0.009044, -0.007548)$, and $r_7 = 128.4$ with CB $(117.4, 139.3)$.

8. General model power-2: $ENT_{HG(G)} = p_8 \cdot HG^{q_8} + r_8$, where the coefficients (with 95% confidence bounds (CB)) are $p_8 = -88.15$ with CB $(-95.55, -80.75)$, $q_8 = -0.01217$ with CB $(-0.01326, -0.01109)$, and $r_8 = 89.96$ with CB $(82.55, 97.37)$.

9. General model power-2: $ENT_{BMG(G)} = p_9 \cdot BMG^{q_9} + r_9$, where the coefficients (with 95% confidence bounds (CB)) are $p_9 = 3221$ with CB $(2923, 3518)$, $q_9 = 0.0003096$ with CB $(0.0002811, 0.0003381)$, and $r_9 = -3222$ with CB $(-3519, -2925)$.

10. General model power-2: $ENT_{BMH(G)} = p_{10} \cdot BMH^{q_{10}} + r_{10}$, where the coefficients (with 95% confidence bounds (CB)) are $p_{10} = -414.9$ with CB $(-451.9, -377.8)$, $q_{10} = -0.002479$ with CB $(-0.002707, -0.002252)$, and $r_{10} = 411.2$ with CB $(374.1, 448.2)$.

11. General model power-2: $ENT_{BMA(G)} = p_{11} \cdot BMA^{q_{11}} + r_{11}$, where the coefficients (with 95% confidence bounds (CB)) are $p_{11} = 4508$ with CB $(4093, 4924)$, $q_{11} = 0.0002213$ with CB $(0.000201, 0.0002417)$, and $r_{11} = -4510$ with CB $(-4926, -4094)$.

12. General model power-2: $ENT_{TMG(G)} = p_{12} \cdot TMG^{q_{12}} + r_{12}$, where the coefficients (with 95% confidence bounds (CB)) are $p_{12} = 2058$ with CB $(1868, 2249)$, $q_{12} = 0.0004835$ with CB $(0.000439, 0.0005281)$, and $r_{12} = -2060$ with CB $(-2251, -1870)$.

13. General model power-2: $ENT_{TMH(G)} = p_{13} \cdot TMH^{q_{13}} + r_{13}$, where the coefficients (with 95% confidence bounds (CB)) are $p_{13} = -272$ with CB $(-295.9, -248.2)$, $q_{13} = -0.003848$ with CB $(-0.0042, -0.003496)$, and $r_{13} = 267.6$ with CB $(243.8, 291.5)$.

14. General model power-2: $ENT_{TMA(G)} = p_{14} \cdot TMA^{q_{14}} + r_{14}$, where the coefficients (with 95% confidence bounds (CB)) are $p_{14} = 7277$ with CB $(6605, 7948)$, $q_{14} = 0.0001372$ with CB $(0.0001246, 0.0001499)$, and $r_{14} = -7279$ with CB $(-7950, -6607)$.

5.2. Zinc silicate network $ZNSL(\alpha)$

1. General model power-2: $ENT_{BM(G)} = p_1 \cdot BM^{q_1} + r_1$, where the coefficients (with 95% confidence bounds (CB)) are $p_1 = 1071$ with CB $(970.3, 1172)$, $q_1 = 0.0009246$ with CB $(0.0008384, 0.001011)$, and $r_1 = -1073$ with CB $(-1174, -972.8)$.

2. General model power-2: $ENT_{TM(G)} = p_2 \cdot TM^{q_2} + r_2$, where the coefficients (with 95% confidence bounds (CB)) are $p_2 = 1942$ with CB $(1760, 2124)$, $q_2 = 0.000512$ with CB $(0.0004643, 0.0005597)$, and $r_2 = -1945$ with CB $(-2127, -1763)$.

3. General model power-2: $ENT_{GBM(G)} = p_3 \cdot GBM^{q_3} + r_3$, where the coefficients (with 95% confidence bounds (CB)) are $p_3 = -798.5$ with CB $(-871.9, -725.2)$, $q_3 = -0.001263$ with CB $(-0.00138, -0.001146)$, and $r_3 = 800$ with CB $(726.7, 873.4)$.

4. General model power-2: $ENT_{GTM(G)} = p_4 \cdot GTM^{q_4} + r_4$, where the coefficients (with 95% confidence bounds (CB)) are $p_4 = -325.6$ with CB $(-355.1, -296.1)$, $q_4 = -0.00313$ with CB $(-0.003418, -0.002842)$, and $r_4 = 327.6$ with CB $(298.1, 357.1)$.

5. General model power-2: $ENT_{GH(G)} = p_5 \cdot GH^{q_5} + r_5$, where the coefficients (with 95% confidence bounds (CB)) are $p_5 = 1760$ with CB $(1595, 1924)$, $q_5 = 0.0005651$ with CB $(0.0005124, 0.0006178)$, and $r_5 = -1762$ with CB $(-1926, -1597)$.

6. General model power-2: $ENT_{HBM(G)} = p_6 \cdot HBM^{q_6} + r_6$, where the coefficients (with 95% confidence bounds (CB)) are $p_6 = -109.5$ with CB $(-119.1, -99.96)$, $q_6 = -0.009552$ with CB $(-0.01042, -0.008686)$, and $r_6 = 112.7$ with CB $(103.2, 122.3)$.

7. General model power-2: $ENT_{HTM(G)} = p_7 \cdot HTM^{q_7} + r_7$, where the coefficients (with 95% confidence bounds (CB)) are $p_7 = -81.59$ with CB $(-88.63, -74.56)$, $q_7 = -0.01294$ with CB $(-0.01411, -0.01178)$, and $r_7 = 85.3$ with CB $(78.26, 92.33)$.

8. General model power-2: $ENT_{HG(G)} = p_8 \cdot HG^{q_8} + r_8$, where the coefficients (with 95% confidence bounds (CB)) are $p_8 = -448.3$ with CB $(-475.1, -421.5)$, $q_8 = -0.002268$ with CB $(-0.002405, -0.00213)$, and $r_8 = 449.1$ with CB $(422.3, 476)$.

9. General model power-2: $ENT_{BMG(G)} = p_9 \cdot BMG^{q_9} + r_9$, where the coefficients (with 95% confidence bounds (CB)) are $p_9 = 1317$ with CB $(1194, 1440)$, $q_9 = 0.0007538$ with CB $(0.0006837, 0.000824)$, and $r_9 = -1318$ with CB $(-1442, -1195)$.

10. General model power-2: $ENT_{BMH(G)} = p_{10} \cdot BMH^{q_{10}} + r_{10}$, where the coefficients (with 95% confidence bounds (CB)) are $p_{10} = -1734$ with CB $(-1894, -1574)$, $q_{10} = -0.0005805$ with CB $(-0.0006346, -0.0005265)$, and $r_{10} = 1731$ with CB $(1570, 1891)$.

11. General model power-2: $ENT_{BMA(G)} = p_{11} \cdot BMA^{q_{11}} + r_{11}$, where the coefficients (with 95% confidence bounds (CB)) are $p_{11} = 1425$ with CB $(1292, 1558)$, $q_{11} = 0.0006971$ with CB $(0.0006322, 0.0007619)$, and $r_{11} = -1427$ with CB $(-1560, -1293)$.

12. General model power-2: $ENT_{TMG(G)} = p_{12} \cdot TMG^{q_{12}} + r_{12}$, where the coefficients (with 95% confidence bounds (CB)) are $p_{12} = 843.5$ with CB $(764, 922.9)$, $q_{12} = 0.001172$ with CB $(0.001062, 0.001281)$, and $r_{12} = -845.5$ with CB $(-925, -766.1)$.

13. General model power-2: $ENT_{TMH(G)} = p_{13} \cdot TMH^{q_{13}} + r_{13}$, where the coefficients (with 95% confidence bounds (CB)) are $p_{13} = -581.5$ with CB $(-634.4, -528.5)$, $q_{13} = -0.001757$ with CB $(-0.00192, -0.001594)$, and $r_{13} = 577.2$ with CB $(524.2, 630.1)$.

14. General model power-2: $ENT_{TMA(G)} = p_{14} \cdot TMA^{q_{14}} + r_{14}$, where the coefficients (with 95% confidence bounds (CB)) are $p_{14} = 862.8$ with CB $(781.6, 944.1)$, $q_{14} = 0.001146$ with CB $(0.001039, 0.001252)$, and $r_{14} = -864.8$ with CB $(-946.1, -783.6)$.

Zagreb-type topological indices	**Data**	**Fit-type**	$\mathbf{R^2}$	**SSE**	**RMSE**
$BM(G)$	$BM(G)$ vs. $ENT_{BM(G)}$	Power-2	1.0000	0.0000	0.0000
$TM(G)$	$TM(G)$ vs. $ENT_{TM(G)}$	Power-2	1.0000	0.0000	0.0001
$GBM(G)$	$GBM(G)$ vs. $ENT_{GBM(G)}$	Power-2	1.0000	0.0000	0.0001
$GTM(G)$	$GTM(G)$ vs. $ENT_{GTM(G)}$	Power-2	1.0000	0.0000	0.0003
$GH(G)$	$GH(G)$ vs. $ENT_{GH(G)}$	Power-2	1.0000	0.0002	0.0022
$HBM(G)$	$HBM(G)$ vs. $ENT_{HBM(G)}$	Power-2	1.0000	0.0000	0.0008
$HTM(G)$	$HTM(G)$ vs. $ENT_{HTM(G)}$	Power-2	1.0000	0.0001	0.0010
$HG(G)$	$HG(G)$ vs. $ENT_{HG(G)}$	Power-2	1.0000	0.0001	0.0015
$BMG(G)$	$BMG(G)$ vs. $ENT_{BMG(G)}$	Power-2	1.0000	0.0000	0.0000
$BMH(G)$	$BMH(G)$ vs. $ENT_{BMH(G)}$	Power-2	1.0000	0.0000	0.0003
$BMA(G)$	$BMA(G)$ vs. $ENT_{BMA(G)}$	Power-2	1.0000	0.0000	0.0000
$TMG(G)$	$TMG(G)$ vs. $ENT_{TMG(G)}$	Power-2	1.0000	0.0000	0.0001
$TMH(G)$	$TMH(G)$ vs. $ENT_{TMH(G)}$	Power-2	1.0000	0.0000	0.0005
$TMA(G)$	$TMA(G)$ vs. $ENT_{TMA(G)}$	Power-2	1.0000	0.0000	0.0001

Table 6: The statistics of curve fitting of Zagreb-type topological indices versus entropy measures of $ZNOX(\alpha)$ for $1 \leq \alpha \leq 100$

Zagreb-type topological indices	Data	Fit-type	R^2	SSE	RMSE
$BM(G)$	$BM(G)$ vs. $ENT_{BM(G)}$	Power-2	1.0000	0.0000	0.0001
$TM(G)$	$TM(G)$ vs. $ENT_{TM(G)}$	Power-2	1.0000	0.0000	0.0001
$GBM(G)$	$GBM(G)$ vs. $ENT_{GBM(G)}$	Power-2	1.0000	0.0000	0.0002
$GTM(G)$	$GTM(G)$ vs. $ENT_{GTM(G)}$	Power-2	1.0000	0.0000	0.0004
$GH(G)$	$GH(G)$ vs. $ENT_{GH(G)}$	Power-2	1.0000	0.0000	0.0001
$HBM(G)$	$HBM(G)$ vs. $ENT_{HBM(G)}$	Power-2	1.0000	0.0001	0.0012
$HTM(G)$	$HTM(G)$ vs. $ENT_{HTM(G)}$	Power-2	1.0000	0.0001	0.0016
$HG(G)$	$HG(G)$ vs. $ENT_{HG(G)}$	Power-2	1.0000	0.0000	0.0002
$BMG(G)$	$BMG(G)$ vs. $ENT_{BMG(G)}$	Power-2	1.0000	0.0000	0.0001
$BMH(G)$	$BMH(G)$ vs. $ENT_{BMH(G)}$	Power-2	1.0000	0.0000	0.0001
$BMA(G)$	$BMA(G)$ vs. $ENT_{BMA(G)}$	Power-2	1.0000	0.0000	0.0001
$TMG(G)$	$TMG(G)$ vs. $ENT_{TMG(G)}$	Power-2	1.0000	0.0000	0.0002
$TMH(G)$	$TMH(G)$ vs. $ENT_{TMH(G)}$	Power-2	1.0000	0.0000	0.0002
$TMA(G)$	$TMA(G)$ vs. $ENT_{TMA(G)}$	Power-2	1.0000	0.0000	0.0002

Table 7: The statistics of curve fitting of Zagreb-type topological indices versus entropy measures of $ZNSL(\alpha)$ for $1 \leq \alpha \leq 100$

6. Pearson correlation coefficient

The degree and direction of a linear relationship between two continuous variables are measured statistically by the Pearson correlation coefficient (r). Perfect positive correlation is represented by a value of $r = 1$, perfect negative correlation by a value of $r = -1$, and no linear relationship by a value of $r = 0$. The range of values for the Pearson correlation coefficient is -1 to 1. The Pearson correlation coefficient (r) is given by

$$r = \frac{\sum(X_i - \overline{X})(Y_i - \overline{Y})}{\sqrt{\sum(X_i - \overline{X})^2 \sum(Y_i - \overline{Y})^2}}, \tag{6.1}$$

where X and Y denote the means of the corresponding variables, while X_i and Y_i indicate individual data points. The denominator of (6.1) scales the covariance between the two variables by the product of their standard deviations, producing a result that ranges from -1 to 1. The numerator calculates the covariance between the two variables. When indices and entropy are associated, the Pearson correlation coefficient determines whether and how they are related. We examine the relationship between a material's internal disorder, measured by entropy, and its structure, represented by indices, by computing the Pearson correlation. According to a high positive value r, the entropy increases as the index value increases and vice versa. A large negative r number, on the other hand, indicates a propensity for one variable to fall as the other increases.

To better understand the strength and direction of the relationships between entropy and various Zagreb-type indices of $ZNOX(\alpha)$ and $ZNSL(\alpha)$, we created a heatmap using Pearson's correlation coefficients, shown in Figures 5 and Figures 6. This heatmap shows the correlation values, helping to identify whether the variables are positively or negatively related. This information is important for understanding how entropy interacts with Zagreb-type topological indices, showing how changes in entropy connect to variations in the indices. This helps us to analyze complex systems and make better decisions. However, more research is often needed to understand the reasons behind these relationships. Our calculations revealed strong correlations between entropy and certain topological indices, highlighting the connection between structural properties and the complexity of $ZNOX(\alpha)$ and $ZNSL(\alpha)$. These findings provide useful information on the material's potential for various applications.

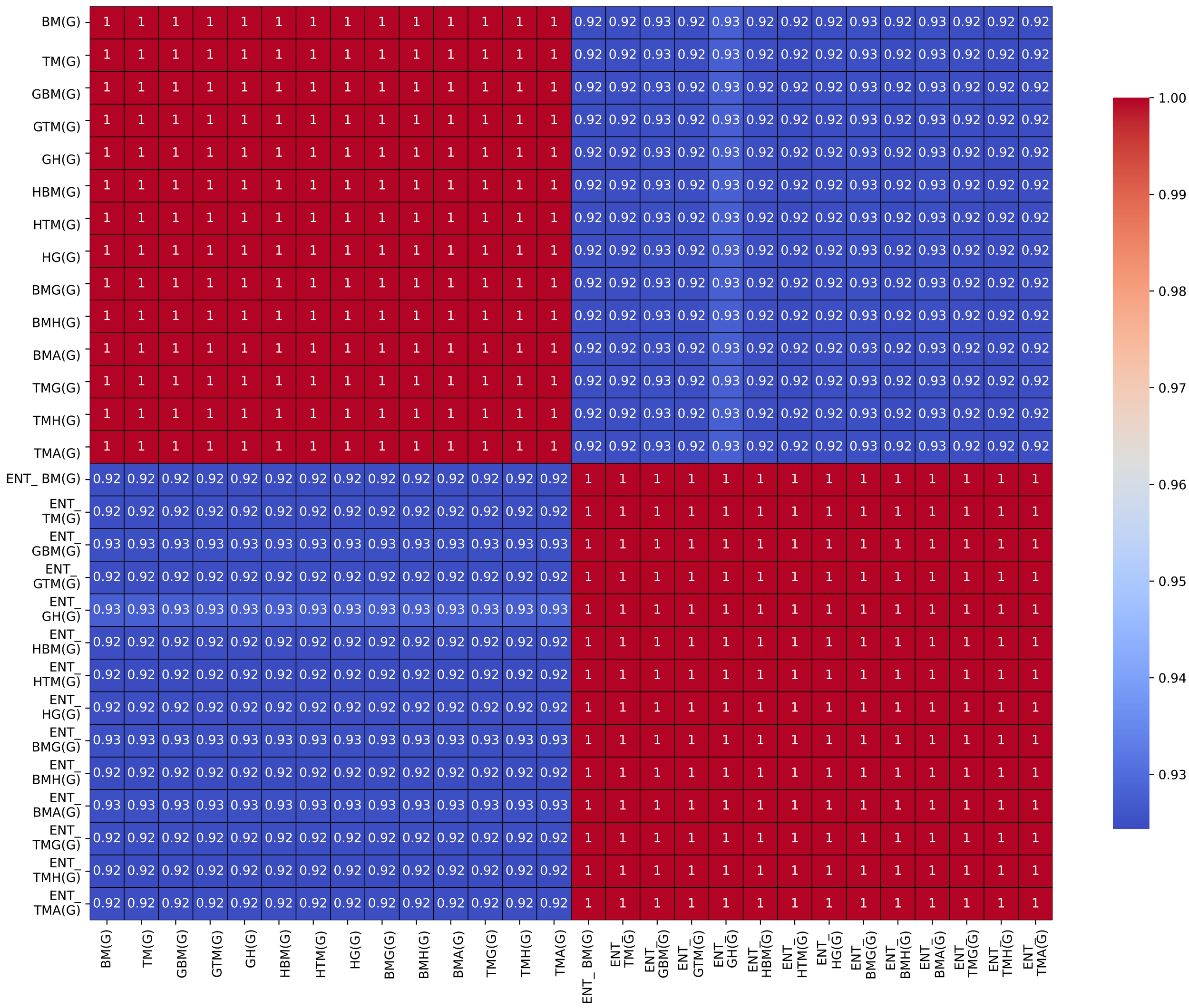

Figure 5: Pearson correlation analysis between Zagreb-type topological indices and entropies of $ZNOX(\alpha)$ for $1 \leq \alpha \leq 100$

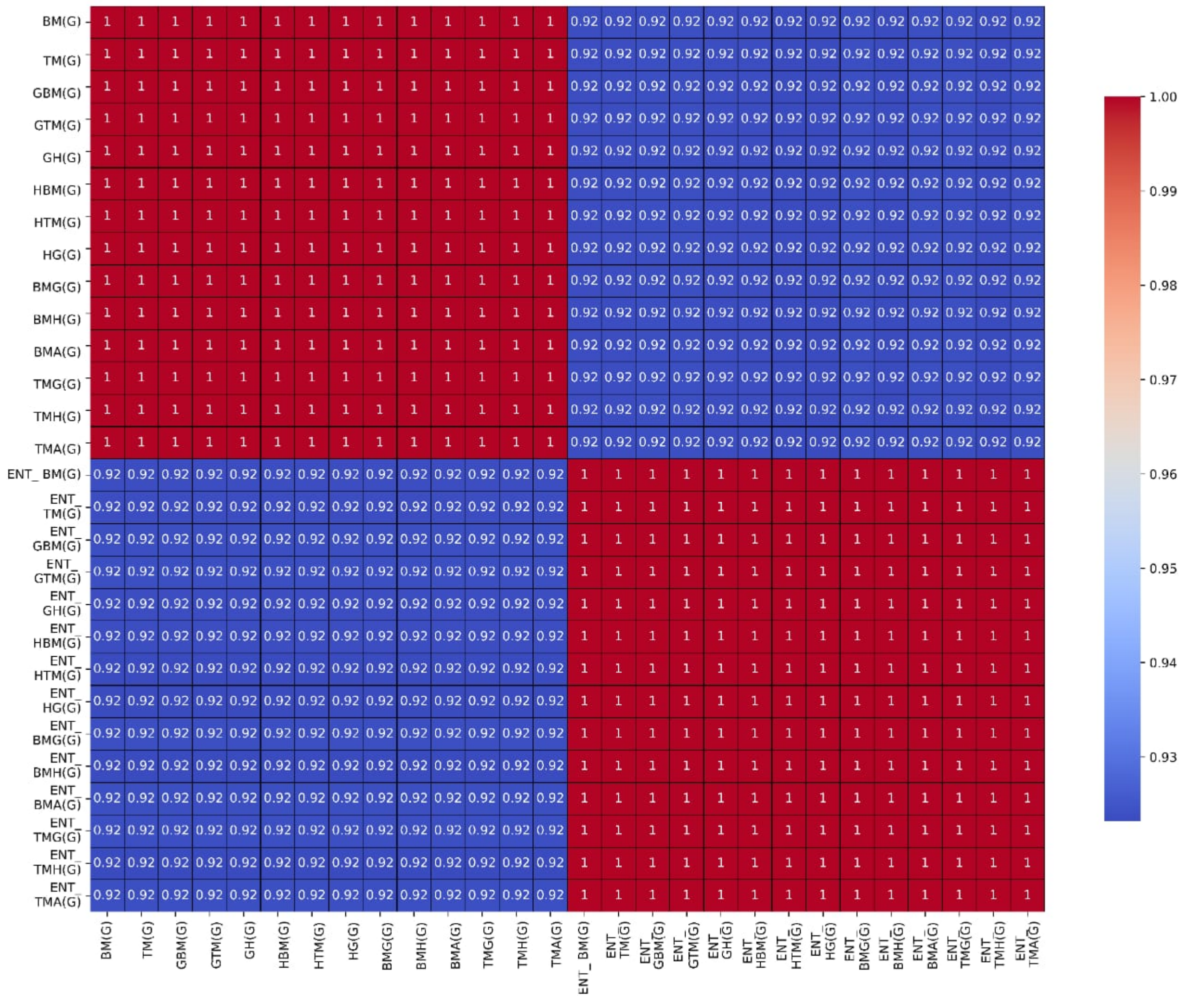

Figure 6: Pearson correlation analysis between Zagreb-type topological indices and entropies of $ZNSL(\alpha)$ for $1 \leq \alpha \leq 100$

7. Conclusion

In this work, we have used edge partition approaches based on the terminal degrees of bonds to construct mathematical formulas for new Zagreb-type topological indices. We investigated entropy measures based on these indices using the Shannon entropy concept. Furthermore, a comparison study using 2-D line plots was carried out, along with the numerical computations and graphical representations of the Zagreb-type indices and their respective entropy measures. According to the results shown in Tables 2 and 3, there are particular correlations between the Zagreb-type indices and their corresponding entropy measures of $ZNOX(\alpha)$ and $ZNSL(\alpha)$, which increase with increasing values of α. Furthermore, curve-fitting models were used to create the best regression models that correlated the Zagreb-type indices with their associated entropies. A correlation analysis was then conducted to assess the interrelationships between the chosen molecular descriptors. The results of this investigation into the topological and structural characteristics of silicate and zinc oxide networks may prove useful in different domains.

The potential limitations of the work: Although this study provides valuable insights into the relationship between Zagreb-type topological indices and their corresponding entropy measures using the Pearson correlation coefficient and the power-2 regression model, it is subject to certain limitations.

Firstly, the analysis was confined to and zinc oxide and silicate networks, which may limit the generalizability of the findings to other network topologies. Future research could extend this approach to a wider variety of chemical networks and graph structures to evaluate the robustness and applicability of novel entropy metrics derived from Zagreb-type indices. Secondly, while the power-2 regression model effectively captured the non-linear relationship between the indices and entropy measures, exploring alternative regression techniques could potentially yield even more accurate or insightful correlations. Finally, this study primarily relied on the Pearson correlation coefficient to assess linear relationships. However, investigating other statistical measures or employing non-linear correlation techniques may offer a deeper and more nuanced understanding of complex data patterns.

Future research will focus on evaluating the predictive ability of the proposed Zagreb-type topological indices and entropy measures in estimating the energetic properties of zinc oxide and silicate networks, such as the HOMO-LUMO gap, π-electron energy, and delocalization energy. This approach has the potential to enhance our understanding of the relationship between molecular topology and energy characteristics, opening new possibilities for applications in materials science and nanotechnology.

Funding

No funding is available for this study.

Author contributions

U. Vijaya Chandra Kumar, H. M. Nagesh: Conceptualization, methodology, and writing-original draft.

Data Availability Statement

This manuscript has no associated data.

Ethical Approval

Not applicable.

Conflict of interests

The authors declare that they have no known competing financial interests or personal relationships that could have appeared to influence the work reported in this paper.

References

1. Z. Hong-Cai, R. Jeffrey, O. M. Yaghi, Introduction to Metal-Organic Frameworks, *Chem. Rev.* **112(2)** (2012) 673–674.

2. G. Pan, M. Soumya, Z. Hussain, et al, Porphyrin-based MOFs for sensing environmental pollutants, *Chemical Engineering Journal.* **492** (2014). doi:10.1016/j.cej.2024.152377. ISSN 1385-8947.

3. S. A. Lisa, S. Philip, H. Dominik, et al, Vectorial Catalysis in Surface-Anchored Nanometer-Sized Metal–Organic Frameworks-Based Microfluidic Devices, *Angewandte Chemie International Edition.* **61(8)** (2022). doi: e202115100. doi:10.1002/anie.202115100.

4. F. Zhiying, S. Lena, H. Karina, et al, Enhanced catalytic performance of palladium nanoparticles in MOFs by channel engineering, *Cell Reports Physical Science.* **3(2)** (2022). doi:10.1016/j.xcrp.2022.100757.

5. S. R. Batten N. R, Champness, et at, Terminology of metal-organic frameworks and coordination polymers (IUPAC Recommendations 2013), *Pure and Applied Chemistry.* **85(8)** (2013) 1715–1724. doi:10.1351/PAC-REC-12-11-20.

6. B. Thomas, C. Anthony, Amorphous Metal-Organic Frameworks, *Accounts of Chemical Research.* **47(5)** (2014) 1555–1562. doi:10.1021/ar5000314.

7. B. Thomas C. François-Xavier, et al, The changing state of porous materials, *Nature Materials.* **20(9)** (2021) 1179–1187. doi:10.1038/s41563-021-00957-w.

8. M. Mon, R. Bruno, J. Ferrando-Soria, et al, Metal-organic framework technologies for water remediation: towards a sustainable ecosystem, *Journal of Materials Chemistry A.* **6(12)** (2018) 4912–4947. doi:10.1039/c8ta00264a.

9. J. Cejka J, *Metal-Organic Frameworks Applications from Catalysis to Gas Storage*, Wiley-VCH, 2011.

10. W. Gao, M. Siddiqui, M. Naeem, N. Rehman, Topological characterization of carbon graphite and crystal cubic carbon structures, *Mol.* **22(9)** (2017) 1496.

11. S. Sharma, V.K. Bhat, S. Lal, The metric resolvability and topological characterization of some molecules in H1N1 antiviral drugs, *Mol. Simul.* **49(11)** (2023) 1165–1178.

12. M.F. Nadeem, M. Azeem, I. Farman, Comparative study of topological indices for capped and uncapped carbon nanotubes, *Polycycl. Aromat. Compd.* **42(7)** (2021) 4666–4683.

13. X. Zhang, S Prabhu, M Arulperumjothi, S. M. Prabhu, M. Arockiaraj, V. Manimozhi, Distance-based topological characterization, graph energy prediction, and NMR patterns of benzene ring embedded in P-type surface in 2D network, *Scientific Reports.* **14(1)** (2024) 23766.

14. Z. Raza, M. Arockiaraj, A. Maaran, S.R.J. Kavitha, K. Balasubramanian, Topological entropy characterization, NMR and ESR spectral patterns of coronene-based transition metal-organic frameworks, *ACS Omega.* **8(14)** (2023) 13371–13383.

15. A. Rajpoot, L. Selvaganesh, Potential application of novel AL indices as molecular descriptors, *J. Mol. Graph. Model.* **118** (2023) 108353.

16. M. Arockiaraj, J.C. Fiona, S.R.J. Kavitha, A.J. Shalini, K. Balasubramanian, Topological and spectral properties of wavy zigzag nanoribbons, *Mol.* **28(1)** (2022) 152.

17. A. Sattar, M. Javaid, Topological aspects of metal-organic frameworks: Zinc silicate and oxide networks, *Computational and Theoretical Chemistry.* **1222** (2023) 114056.

18. M. T. Hussain, M. Javaid, U. Ali, A. Raza, Md Nur Alam, Comparing zinc oxide- and zinc silicate-related metal-organic networks via connection-based Zagreb indices, *Journal of Chemistry.* **2021**. https://doi.org/10.1155/2021/5066394.

19. M. Javaid, A. Sattar, On topological indices of zinc-based metal-organic frameworks, *Main Group Metal Chemistry.* **45** (2022) 74–85.

20. V. Ravi, K. Desikan, N. Chidambaram, On the computation of neighborhood degree sum-based topological indices for zinc-based metal-organic frameworks, *Main Group Metal Chemistry* **46**(2023) 20228043.

21. R. Huang, M.F. Hanifb, M.K. Siddiqui, M.F. Hanif, On analysis of entropy measure via logarithmic regression model and Pearson correlation for Tri-s-triazine, *Computational Materials Science.* **240** (2024) 112994.

22. M. Arockiaraj, J. C. Fiona, A. J. Shalini, Comparative study of entropies in silicate and oxide frameworks, *Silicon* **16** (2024) 3205–3216. https://doi.org/10.1007/s12633-024-02892-2.

23. C.E. Shannon, A mathematical theory of communication, *Bell Syst. Tech. J.* **27** (1948) 379-423.

24. N. Rashevsky, Life, information theory, and topology, *Bull. Math. Biol.* **17** (1955) 229-235.

25. M.M. Dehmer, M. Graber, The discrimination power of molecular identification numbers revisited, *MATCH Commun. Math. Comput. Chem.* **69** (2013) 785-794.

26. A. Mowshowitz, M. Dehmer, Entropy and the complexity of graphs revisited, Entropy. **14** (2012) 559-570.

27. S. Cao, M. Dehmer, Degree-based entropies of networks revisited, *Appl.Math.Comput.* **261** (2015) 141-147.

28. S. Cao, M. Dehmer, Y. Shi, Extremality of degree-based graph entropies. *Inf.Sci.* **278** (2014) 22-33.

29. M. Dehmer, L. Sivakumar, K. Varmuza, Uniquely discriminating molecular structures using novel eigenvalue-based descriptors, *MATCH Commun. Math. Comput. Chem.* **67** (2012) 147-172.

30. E. Estrada, N. Hatano, Statistical-mechanical approach to subgraph centrality in complex networks. *Chem.Phys.Lett.* **439** (2007) 247-251.

31. E. Estrada, Generalized walks-based centrality measures for complex biological networks. *J.Theor.Biol.* **263** (2010) 556-565.

32. D.S. Sabirov, I.S. Shepelevich, Information entropy in chemistry: an overview, *Entropy.* **23(10)** (2021) 1240.

33. R. Kazemi, Entropy of weighted graphs with the degree-based topological indices as weights, *MATCH Commun. Math. Comput. Chem.* **76** (2016) 69-80.

34. M.P. Rahul, Joseph Clement, et al. Degree-based entropies of graphene, graphyne and graphdiyne using Shannon's approach, *Journal of Molecular Structure*, **1210** (2022) 132797. https://doi.org/10.1016/j.molstruc.2022.132797.

U. Vijaya Chandra Kumar,

Department of Mathematics,

School of Applied Sciences, REVA University,

India.

E-mail address: `uvijaychandra.kumar@reva.edu.in`

and

H. M. Nagesh,

Department of Science & Humanities, PES University,

India.

E-mail address: `nageshhm@pes.edu`